Reducing false positives in tractography with microstructural and anatomical priors

Simona Schiavi[1] , Muhamed Barakovic[2] , Mario Ocampo-Pineda[1] , Maxime Descoteaux[4] , Jean-Philippe Thiran[2,3], and Alessandro Daducci[1,*]

[1]Computer Science department, University of Verona, Italy
[2]Signal Processing Lab (LTS5), École Polytechnique Fédérale de Lausanne, Switzerland
[3]University Hospital Center (CHUV) and University of Lausanne (UNIL), Switzerland
[4]Sherbrooke Connectivity Imaging Lab (SCIL), Université de Sherbrooke, Canada
[*]Corresponding author: alessandro.daducci@univr.it

Abstract

Tractography is a family of algorithms that use diffusion-weighted magnetic resonance imaging data to reconstruct the white matter pathways of the brain. Although it has been proven to be particularly effective for studying non-invasively the neuronal architecture of the brain, recent studies have highlighted that the large incidence of false positive connections retrieved by these techniques can significantly bias any connectivity analysis. Some solutions have been proposed to overcome this issue and the ones relying on convex optimization framework showed a significant improvement. Here we propose an evolution of the Convex Optimization Modeling for Microstructure Informed Tractography (COMMIT) framework, that combines basic prior knowledge about brain anatomy with group-sparsity regularization into the optimization problem. We show that the new formulation dramatically reduces the incidence of false positives synthetic data.

1 Introduction

Diffusion-weighted magnetic resonance imaging (DW-MRI) is a non-invasive imaging technique that is sensitive to how water diffuses in tissues [1]. Based on the directionality retrieved from water diffusion inside white matter (WM), tractography algorithms can infer the major neuronal pathways of brain [2]. Over the years, tractography has proven particularly effective for studying non-invasively the neuronal architecture of the brain, both in healthy subjects [3] as well as for investigating a wide range of neurological conditions [4]. However, recent studies have challenged its use for connectivity analyses, notably showing that the presence of false positive connections in the reconstructions can significantly bias the topological properties of the estimated brain networks [5–7]. The major limitation is that, because of the significant difference between DW-MRI data resolution (order of millimeters) and the size of the axons (order of micrometers), a single tract reconstructed with tractography cannot represent a single axon, but rather a coherent set of real anatomical fibers. Recent studies have highlighted how this limitation affects the accuracy of tractography reconstructions even when using very high quality data [8, 9]. This results in an intrinsic trade-off between sensitivity, i.e. capability of reconstructing real WM bundles, and specificity, i.e. retrieving only true connections. Using topological properties of the structural network built from the tractogram, Zalesky et al. have shown that specificity is at least twice as important as sensitivity [6]. False positive streamlines dramatically bias any connectivity

analysis, as non-existent structures are mixed with real ones. To overcome these issues, a number of solutions have been proposed recently to combine tractography with local microstructural DW-MRI features for mapping connectivity [10]. Among those, "Spherical-deconvolution informed filtering of tractograms" (SIFT [11] and SIFT2 [12]), "linear fascicle evaluation" (LIFE [13]) and Convex Optimization Modeling for Microstructure Informed Tractography (COMMIT[14, 15]) have shown the ability to remove some implausible positive connections by making the streamlines more quantitative. All this method are data driven. They consider the streamlines as quantitative independent entities and evaluate the effective contribution of those to the DW-MRI signal.

In this study, we present a novel processing framework that can dramatically reduce the incidence of these false positives, i.e. improving specificity, without affecting the true ones, i.e. sensitivity. Tractography algorithms usually exploit only the directional information estimated with diffusion MRI: we speculate that this information is not enough and we advocate the need for additional data to help tractography producing more accurate reconstructions. Our formulation combines basic prior knowledge about brain anatomy with group-sparsity regularization into an efficient convex optimization problem. We evaluated quantitatively the effectiveness of our formulation on different tractography reconstructions using a realistic digital phantom with known ground-truth.

2 Materials and methods

2.1 Microstructure Informed Tractography

The Convex Optimization Modeling for Microstructure Informed Tractography (COMMIT) [14, 15] is a framework that allows to supplement microstructural information to every streamline in a tractogram. Given a tractogram $\mathcal{T}$, the corresponding DW-MRI image $\mathbf{I} \in \mathbb{R}_+^{n_x \times n_y \times n_z \times n_d}$, is composed of n_d q-space samples acquired for $n_v = n_x n_y n_z$ voxels, and can be defined as $\mathbf{I} = \mathcal{A}(\mathcal{T}) + \eta$, where $\mathcal{A} : \mathcal{T} \rightarrow \mathbf{I}$ is an operator describing the signal contribution of each fiber in all the imaging voxels and η is a function that accounts for acquisition's noise. The general aim of all the tractography algorithms is to solve the inverse problem of finding the set of streamlines $\tilde{\mathcal{T}}$ that best describe the input DW-MRI data. COMMIT framework, instead, receives as input any tractogram $\mathcal{T}$ (built with any available algorithm) along with the corresponding DW-MRI image $\mathbf{I}$ and finds the candidate $\tilde{\mathcal{T}}$ by solving a global convex optimization problem. The observation model is given by

$$\mathbf{y} = \mathbf{A}\mathbf{x} + \eta \tag{1}$$

where $\mathbf{y} \in \mathbb{R}_+^{n_d n_v}$ is the vector containing the n_d q-space samples acquired in all n_v voxels, η accounts for both acquisition noise and modeling errors, $\mathbf{A} \in \mathbb{R}^{n_d n_v \times n_c}$ is the observation matrix (i.e. dictionary) modeling explicitly the predefined multicompartment model in every voxel and the positive weights $\mathbf{x} \in \mathbb{R}_+^{n_c}$ are the contributions of the n_c basis functions of $\mathbf{A}$ (i.e. atoms).

In general a multi-compartment model assumes different diffusion behaviors according to the microstructure geometrical properties. A common assumption is to distinguish between three compartments [16]: intra-axonal (IA, mimicking the restricted movement of the water inside the axons), extra-axonal (EA, mimicking the hindered movement of the water outside the axons) and isotropic (ISO, mimicking the free movement of the water like in CSF). The linear operator $\mathbf{A}$ is then a block matrix:

$$\mathbf{A} = \left[\begin{array}{c|c|c} \mathbf{A}^{\mathsf{IA}} & \mathbf{A}^{\mathsf{EA}} & \mathbf{A}^{\mathsf{ISO}} \end{array} \right], \tag{2}$$

where $n_c = n_r + n_h + n_i$ and the sub-matrices $\mathbf{A}^{\mathsf{IA}} \in \mathbb{R}^{n_d n_v \times n_r}$, $\mathbf{A}^{\mathsf{EA}} \in \mathbb{R}^{n_d n_v \times n_h}$ and $\mathbf{A}^{\mathsf{ISO}} \in \mathbb{R}^{n_d n_v \times n_i}$ encode, respectively, the n_r restricted, n_h hindered and n_i isotropic contributions to the image. The contributions $\mathbf{x}$ of all the compartments can be estimated by solving the following

non-negative least-square (NNLS) problem:

$$\underset{\mathbf{x}\geq 0}{\operatorname{argmin}} \, ||\mathbf{A}\mathbf{x} - \mathbf{y}||_2^2 \,, \tag{3}$$

where $||\cdot||_2$ is the Euclidean norm in $\mathbb{R}^n$.

2.2 Illustrative toy example

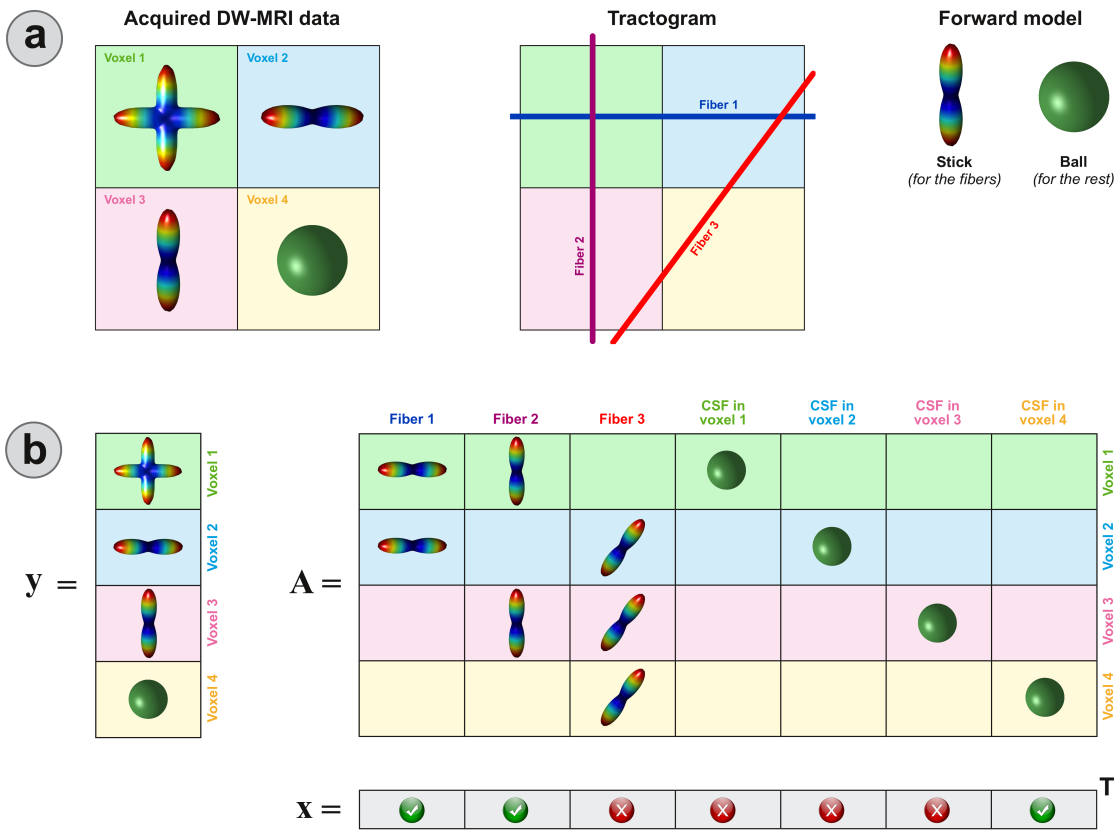

Figure 1: Synthetic toy example to illustrate the modeling and the parameter estimation using the COMMIT framework. (**a**) The simulated DW-MR data, a possible tractogram estimated with a generic tractography algorithm and the forward-model used to associate a signal contribution to each streamline. (**b**) The corresponding vector $\mathbf{y}$ containing all the DW-MR measurements, the matrix $\mathbf{A}$ encoding the signal contributions to DW-MR image according to the chosen forward-model of each streamline (as well as potential presence of CSF) and the coefficients $\mathbf{x}$ estimated by COMMIT. For the sake of simplifying the presentation, diffusion profiles (ODFs) are visualized instead of the actual DW signals.

To illustrate this estimation process, consider the simple toy example shown in Fig. 1**a**. The input tractogram consists of three streamlines that have been reconstructed, with a generic tractography algorithm, from the 2×2 voxels DW-MRI dataset on the left, which shows the diffusion profiles (ODFs) corresponding to each voxel; for this example we use a simple 2-compartment model [REF]. to fit the measured signal (Fig. 1c), we would like to filter out false

positives from the tractogram, i.e. the red line (labelled as Fiber 3). We store the measured signal in the column vector $\mathbf{y}$, where each line contains the signal of each voxel from 1 to 4. To build $\mathbf{A}$, we start checking which voxels are crossed by fiber 1. From 1b we see that it is oriented horizontally and it passes through voxels 1 and 2. So in column one of $\mathbf{A}$, we assign the value of the response function given by an horizontal stick to these two voxels, while we assign 0 to the others. In the same manner, for fiber 2 (column 2 of $\mathbf{A}$), we assign the value of the response function given by a vertical stick to voxels 1 and 3 and 0 the other two, while for fiber 3 we assign the value of the response function given by a 45°rotated stick to voxels 2, 3 and 4, and 0 to voxel 1. To complete the matrix we will then add a column for each voxel that will take into account the presence of isotropic diffusion in that compartment, that is a block for which all the entries are 0 except for the diagonal ones which contains the signal modelled by a ball. Running COMMIT means find the appropriate values for the column vector $\mathbf{x}$ such that $\mathbf{y} = \mathbf{A}\mathbf{x}$. Making the standard multiplication matrix by vector, we have that

- to obtain the fist value of $\mathbf{y}$ the first two entries of $\mathbf{x}$ must be equal to 1 while the fourth must be 0;
- to obtain the second value of $\mathbf{y}$ the first entries of $\mathbf{x}$ must be equal to 1 while the third and the fifth must be 0;
- to obtain the third value of $\mathbf{y}$ the second entries of $\mathbf{x}$ must be equal to 1 while the third and the sixth must be 0;
- to obtain the fourth value of $\mathbf{y}$ the seventh entries of $\mathbf{x}$ must be equal to 1 while the third must be 0.

In this way, the entries of $\mathbf{x}$ are uniquely determined and, since the third is equal to 0, the third streamline will be marked as false positive and removed from the tractogram.

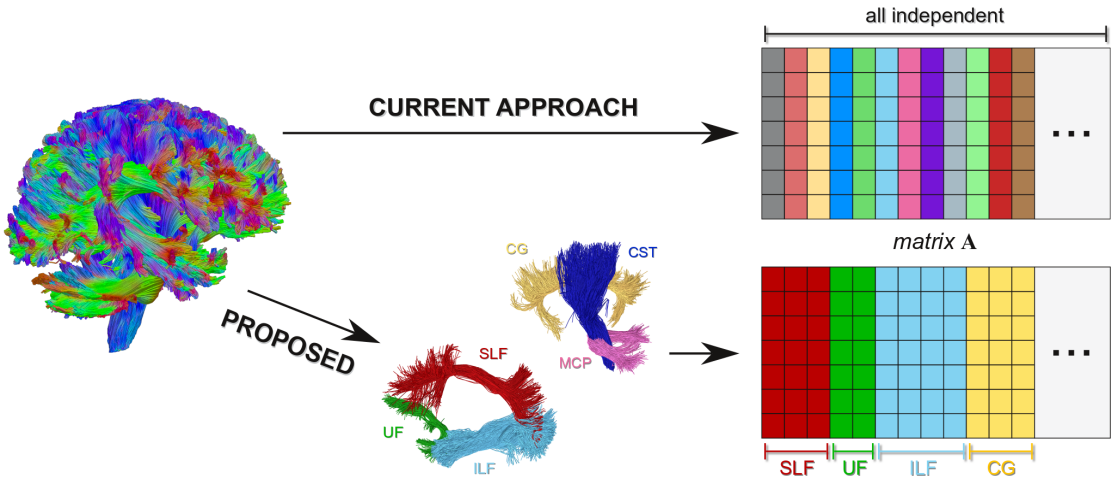

Figure 2: Illustration of the novel prior added in the proposed method. While the current approach (COMMIT) builds the model matrix A by treating each streamlines independently (one streamlines is modeled by one column), the proposed approach (COMMIT2) groups the streamlines of the same bundle together and considers them as unique entity for the optimization (one streamline is modeled by one column but streamlines of the same bundle are grouped together as sub-block of the matrix).

2.3 Injecting priors about brain anatomy and its organization

In some cases the DW-MRI signal can be very ambiguous and the resulting tractogram might contain configurations of fibers that are compatible with the DW-MRI signal, but not with the underlying anatomy. For this reason, we extended COMMIT by adding a constraint which takes into account that axons in white matter are generally organized in bundles. To mathematically translate this, we changed the regularization term in the NNLS problem using *group lasso* [17] formulation instead of the standard *lasso*. In this way, we penalize the contributions at the level of groups and in practice we search the solution that explain the signal with the minimum number of groups (i.e. bungles). Thus, the problem 3 becomes

$$\underset{\mathbf{x}\geq 0}{\text{argmin}}\ ||\mathbf{A}\mathbf{x}-\mathbf{y}||_2^2\ +\ \lambda \sum_{g\in\mathcal{G}} ||\mathbf{x}^{(g)}||_2 \tag{4}$$

where $\mathcal{G}$ represents a general partition of the streamlines into groups. Without any strong a priori knowledge on the bundles, a classical way to operatively solve this problem is to use the so called *adaptive group lasso* [18] which penalises all the groups in the same manner independently of their size. The new problem can then be rewritten as

$$\underset{\mathbf{x}\geq 0}{\text{argmin}}\ ||\mathbf{A}\mathbf{x}-\mathbf{y}||_2^2\ +\ \sum_{g\in\mathcal{G}} \lambda^{(g)}\, ||\mathbf{x}^{(g)}||_2 \tag{5}$$

with

$$\lambda^{(g)} = \frac{\lambda\sqrt{|g|}}{||\mathbf{x}^{(g)}_{\text{NNLS}}||_2} \tag{6}$$

where λ is a regularization parameter to be set, $|g|$ is the cardinality of the group g and $||\mathbf{x}^{(g)}_{\text{NNLS}}||_2$ are the weights of the streamlines obtained by solving the NNLS problem in 3.

2.4 Numerical simulations

We quantitatively evaluated our proposed approach using the simulated dataset that was built for the Reconstruction Challenge organized in 2013 at the IEEE International Symposium on Biomedical Imaging (ISBI). This synthetic phantom was created using the Phantomas simulator [19] and consists of 27 ground-truth fiber bundles designed to mimic the highest challenges encountered by tractography algorithms in the brain i.e. branching, kissing, crossing fiber bundles at angles between 30°and 90°, with various bundle curvature and size. The corresponding DW-MRI signal was generated according to the CHARMED model [20], along 64 directions with $b = 3000\text{s/mm}^2$ and Rician noise with a signal-to-noise ratio (SNR) of 30. To define the GM ROIs, we labeled the voxels at the extremity or the WM mask with 53 different values representing one GM ROI each.

2.4.1 Evaluation criteria

To assess the sensitivity and the specificity of a connectome, we used the Tractometer metrics defined in [21]. True positives (TP) are described in terms of the *Valid Connections* (VC) ratio, which is the proportion of streamlines in the tractogram that connect a correct pair of ROIs, as well as the corresponding number of *Valid Bundles* (VB). Similar metrics can be computed for the false positives (FP), i.e. *Invalid Connections* (IC) and *Invalid Bundles* (IB). To summarize sensitivity and specificity in a single score, we computed the *Youden's index* defined as $J = \text{sensitivity} + \text{specificity} - 1$. Sensitivity is defined as the ratio between VB and the number

of real positives (27 in this dataset), and the specificity as the ratio between 1-IB and the number of real negative (462 in this dataset); this value represent the number of pairs of ROIs that may potentially be connected (incorrectly) and was computed by reconstructing 10 million streamlines with probabilistic tractography.

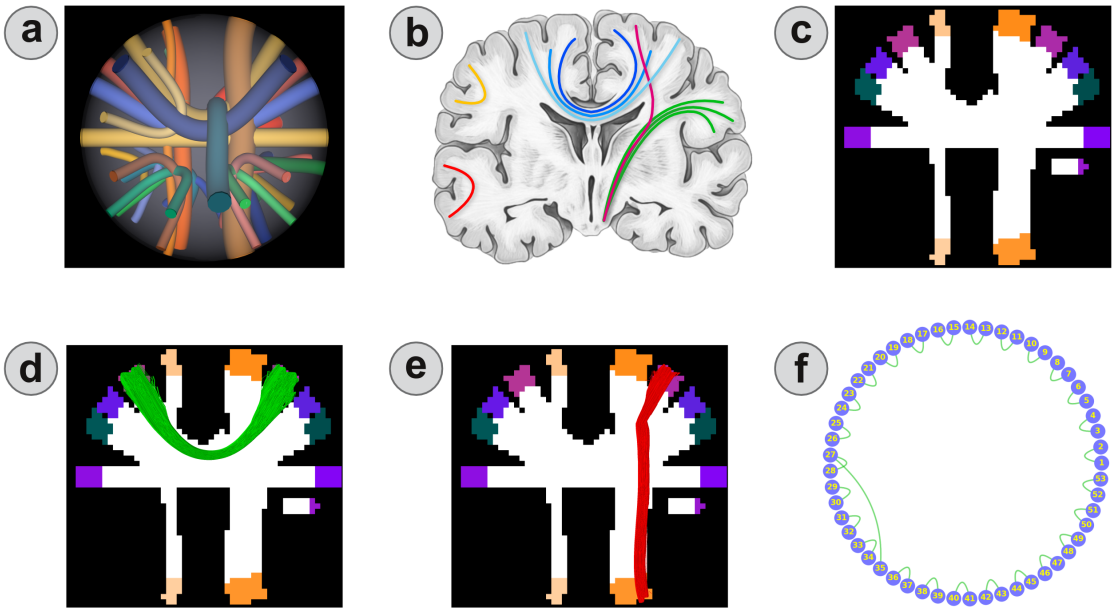

Figure 3: Synthetic dataset used to quantitatively evaluate our method (**a**), inspired from real anatomical bundles of the human brain (**b**). White-matter and gray-matter masks used for tractography (**c**). Examples of True Positive (TP, **d**) and False Positive (FP, **e**) bundles extracted by tractography. Ground-truth connectivity represented as a graph (**f**): TP and FP are represented, respectively, as green and red arcs (no FP are present in the ground-truth).

2.5 Generating tractograms and connectomes

Fiber tracking was performed using MRtrix [22]. We first computed the WM fiber orientation distributions using constrained spherical deconvolution algorithm [23] and then we performed probabilistic tracking with the iFOD2 algorithm [24] and the WM mask as seed region. We generated up to 1 millions streamlines and default iFOD2 parameters. We then used the 53 GM ROIs to generate the connectomes.

2.6 Estimating the intra axonal volume fraction using spherical mean technique

Among all the existing models to estimate the voxel-wise intra axonal signal fraction, we decided to employ the spherical mean techniques (SMT) [25, 26]. We acknowledge that this choice is arbitrary but we believe it does not effect the validity of our framework. Indeed, to improve the microstructure model is out of the scope of COMMIT, although it is important to choose one that has been proven to be valid for the DW-MRI data regime identified by the acquisition's parameters. We performed the fitting with the open source code available at https://github.com/ekaden/smt

.From the output maps we selected the one corresponding to the intra-neurite volume fraction, we masked it with the WM binary mask and we used it to build the operator **A** of the framework.

3 Results and discussion

Fig. 4 analyzes the quality of the reconstructions obtained using the proposed method. In the first row are reported the number of Valid and Invalid bundles (VB and IB respectively) obtained by varying the regularization strength. As expected the number of IB decreases fast for small values of the regularization parameter λ and when it reaches a comparable value with VB the rate of descent decreases. Moreover, by increasing to much λ also the number of VB starts to decrease, because, as it is known in optimization theory, when λ is to big everything should be discarded. In the second row, the Youden's index and the percentage of valid connections (VC) are reported always as function of the regularization strength. While the VC's percentage has an increasing trend till the maximum values of lambda, the Youden's index reaches a maximum in correspondence of the optimal value for λ and then start to decrease as λ continues to increase.

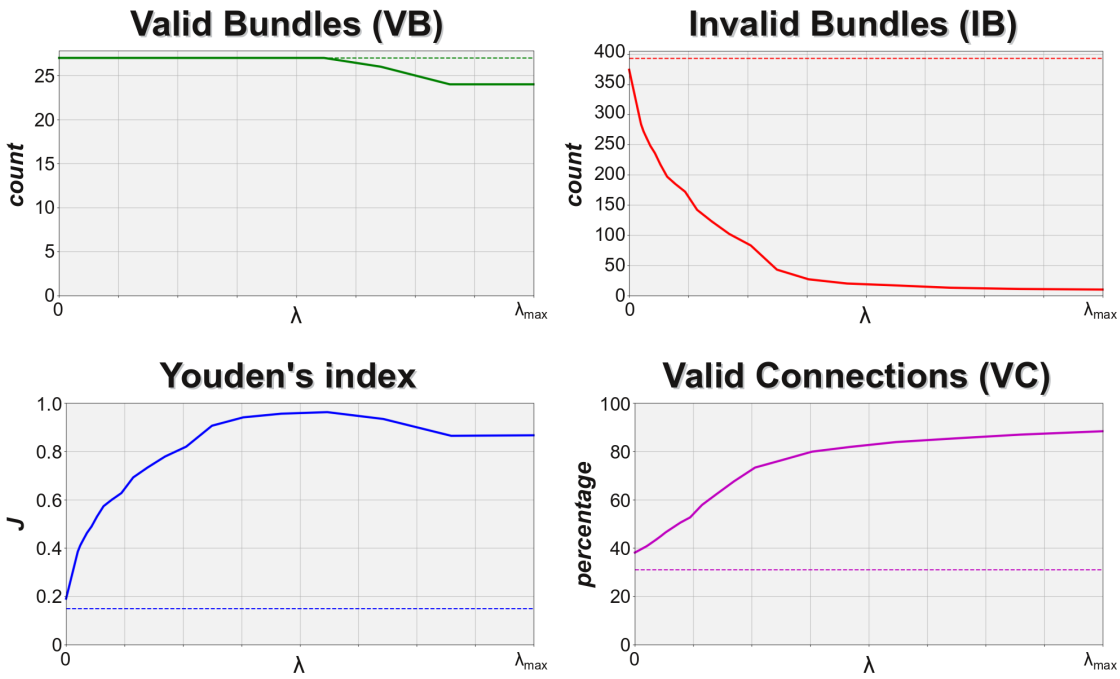

Figure 4: Results obtained using the synthetic dataset. In the first row are reported the number of valid (VB) and invalid (IB) bundles as function of the regularization strength (λ). In the second row are reported the Youden's index and the percentage of valid connections (VC) always as function of λ.

Fig. 5 reports the number of Valid Bundles (VB) and Invalid Bundles (IB) bundles in the raw tractogram. We can easily see that the tracking algorithm was able to reconstruct all 27 TP, i.e. high sensitivity, but at the price of recovering 393 FP, i.e. very low specificity. This result agrees with previous literature [5–7]. On the other hand, Fig. 5B clearly shows that using COMMIT the number of FP can be dramatically reduced (from 393 to 20) without affecting the sensitivity (the tractogram still contains all 27 TP).

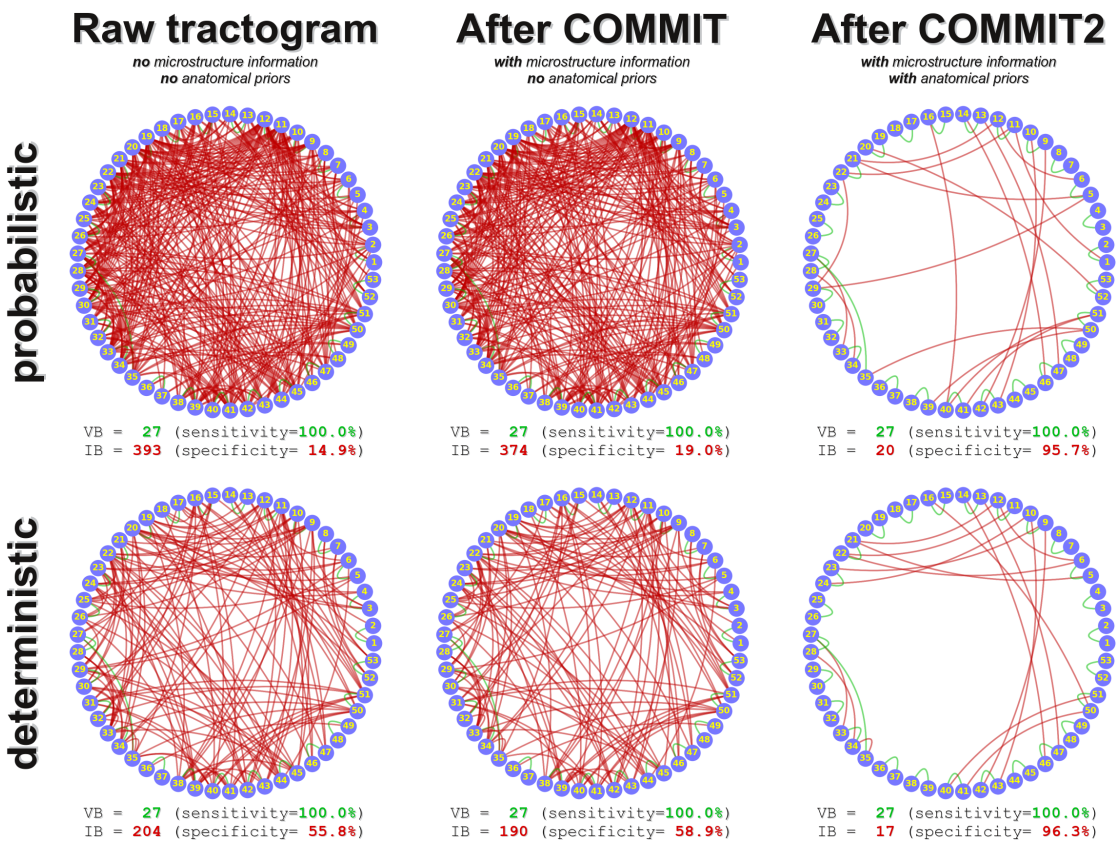

Figure 5: Sensitivity and specificity of a tractogram before (**A**) and after (**B**) applying the proposed method. In both plots, we identify the true positives in "green" and the false positives in "red". Please note that before applying COMMIT the raw tractogram contained TP=27 and FP=235 (the true positives are barely visible) whereas after COMMIT the tractogram still contained all the 27 TP but the FP were dramatically decreased from 235 to 18. Results hold also for other combinations of tracking method and parameters.

3.1 Limitations and future work

This new regularization at the level of bundles guarantees that if a bundle is necessary to explain the signal, then all the streamlines of that bundle will be kept. So, if one has a priori knowledge either from anatomy, either from other methodologies, the regularization parameters $\lambda^{(g)}$ could be set consequently. For example, if we know that a connection surely exists we can promote the corresponding group by setting $\lambda^{(g)} = 0$. On the contrary if we are sure that a connection is not plausible we can set the corresponding $\lambda^{(g)}$ to a very high number which translate in penalizing this group more than the others in the connectome.

4 Conclusion

Recent studies have shown that current tractography algorithms are quite good at reconstructing the major WM bundles, i.e. high sensitivity, but at the price of also recovering a high incidence

of false positive ones, i.e. low specificity. In particular, those false positive streamlines can dramatically bias any subsequent analysis, as non-existent structures are mixed with real ones. In this work, we showed that adding basic prior information on the organization of the neuronal connections can help tractography in dramatically improving the quality of reconstructions. Our results represent an important step forward to improve the accuracy of tractography and may have profound implications for the use of tractography to study brain connectivity.

Acknowledgements

This work was supported by the Rita Levi Montalcini Programme for young researchers of the Italian Ministry of Education, University and Research (MIUR).

References

[1] H. Johansen-Berg and T. E. J. Behrens, *Diffusion MRI: From Quantitative Measurement to In vivo Neuroanatomy.* Elsevier Science, 2013.

[2] P. J. Basser, S. Pajevic, C. Pierpaoli, J. Duda, and A. Aldroubi, "In vivo fiber tractography using DT-MRI data," *Magnetic Resonance in Medicine*, vol. 44, no. 4, pp. 625–632, 2000.

[3] B. Jeurissen, M. Descoteaux, S. Mori, and A. Leemans, "Diffusion MRI fiber tractography of the brain," *NMR in Biomedicine*, 2017.

[4] A. Griffa, P. S. Baumann, J.-P. Thiran, and P. Hagmann, "Structural connectomics in brain diseases," *NeuroImage*, vol. 80, pp. 515–26, 2013.

[5] C. Thomas, F. Ye, O. Irfanoglu, P. Modi, K. Saleem, D. Leopold, and C. Pierpaoli, "Anatomical accuracy of brain connections derived from diffusion MRI tractography is inherently limited," *Proceedings of the National Academy of Sciences of the United States of America*, vol. 111, no. 46, pp. 16574–9, 2014.

[6] A. Zalesky, A. Fornito, L. Cocchi, L. L. Gollo, M. P. van den Heuvel, and M. Breakspear, "Connectome sensitivity or specificity: which is more important?," *NeuroImage*, vol. 142, pp. 407–20, 2016.

[7] K. H. Maier-Hein, P. F. Neher, J.-C. Houde, M.-A. Côté, E. Garyfallidis, J. Zhong, M. Chamberland, F.-C. Yeh, Y.-C. Lin, Q. Ji, W. E. Reddick, J. O. Glass, D. Q. Chen, Y. Feng, C. Gao, Y. Wu, J. Ma, H. Renjie, Q. Li, C.-F. Westin, S. Deslauriers-Gauthier, J. O. O. González, M. Paquette, S. St-Jean, G. Girard, F. Rheault, J. Sidhu, C. M. W. Tax, F. Guo, H. Y. Mesri, S. Dávid, M. Froeling, A. M. Heemskerk, A. Leemans, A. Boré, B. Pinsard, C. Bedetti, M. Desrosiers, S. Brambati, J. Doyon, A. Sarica, R. Vasta, A. Cerasa, A. Quattrone, J. Yeatman, A. R. Khan, W. Hodges, S. Alexander, D. Romascano, M. Barakovic, A. Auría, O. Esteban, A. Lemkaddem, J.-P. Thiran, H. E. Cetingul, B. L. Odry, B. Mailhe, M. S. Nadar, F. Pizzagalli, G. Prasad, J. E. Villalon-Reina, J. Galvis, P. M. Thompson, F. D. S. Requejo, P. L. Laguna, L. M. Lacerda, R. Barrett, F. Dell'Acqua, M. Catani, L. Petit, E. Caruyer, A. Daducci, T. B. Dyrby, T. Holland-Letz, C. C. Hilgetag, B. Stieltjes, and M. Descoteaux, "The challenge of mapping the human connectome based on diffusion tractography," *Nature communications*, vol. 8, no. 1, p. 1349, 2017.

[8] S. Jbabdi and H. Johansen-Berg, "Tractography: where do we go from here?," *Brain connectivity*, vol. 1, no. 3, pp. 169–183, 2011.

[9] K. G. Schilling, V. Nath, C. Hansen, P. Parvathaneni, J. Blaber, Y. Gao, P. Neher, D. B. Aydogan, Y. Shi, M. Ocampo-Pineda, S. Schiavi, A. Daducci, G. Girard, M. Barakovic, J. Rafael-Patino, D. Romascano, G. Rensonnet, M. Pizzolato, A. Bates, E. Fischi, J. P. Thiran, E. J. Canales-Rodríguez, C. Huang, H. Zhu, L. Zhong, R. Cabeen, A. W. Toga, F. Rheault, G. Theaud, J. C. Houde, J. Sidhu, M. Chamberland, C. F. Westin, T. B. Dyrby, R. Verma, Y. Rathi, M. O. Irfanoglu, C. Thomas, C. Pierpaoli, M. Descoteaux, A. W. Anderson, and B. A. Landman, "Limits to anatomical accuracy of diffusion tractography using modern approaches," *NeuroImage*, 2019.

[10] A. Daducci, A. Dal Palú, M. Descoteaux, and J.-P. Thiran, "Microstructure informed tractography: Pitfalls and open challenges," *Frontiers in Neuroscience*, 2016.

[11] R. E. Smith, J. D. Tournier, F. Calamante, and A. Connelly, "SIFT: Spherical-deconvolution informed filtering of tractograms," *NeuroImage*, 2013.

[12] R. E. Smith, J. D. Tournier, F. Calamante, and A. Connelly, "SIFT2: Enabling dense quantitative assessment of brain white matter connectivity using streamlines tractography," *NeuroImage*, 2015.

[13] F. Pestilli, J. D. Yeatman, A. Rokem, K. N. Kay, and B. A. Wandell, "Evaluation and statistical inference for human connectomes," *Nature Methods*, 2014.

[14] A. Daducci, A. Dal Palu, A. Lemkaddem, and J.-P. Thiran, "A convex optimization framework for global tractography," in *ISBI*, pp. 524–27, 2013.

[15] A. Daducci, A. Dal Palù, A. Lemkaddem, and J.-P. Thiran, "COMMIT: Convex optimization modeling for microstructure informed tractography," *IEEE transactions on medical imaging*, vol. 34, no. 1, pp. 246–57, 2015.

[16] A. Sherbondy, M. Rowe, and D. Alexander, "MicroTrack: An Algorithm for Concurrent Projectome and Microstructure Estimation," in *Proc. MICCAI*, pp. 183–90, 2010.

[17] M. Yuan and Y. Lin, "Model selection and estimation in regression with grouped variables," *Journal of the Royal Statistical Society: Series B (Statistical Methodology)*, vol. 68, no. 1, pp. 49–67, 2006.

[18] H. Wang and C. Leng, "A note on adaptive group lasso," *Computational Statistics & Data Analysis*, vol. 52, no. 12, pp. 5277–86, 2008.

[19] E. Caruyer, A. Daducci, M. Descoteaux, J.-C. Houde, J.-P. Thiran, and R. Verma, "Phantomas: a flexible software library to simulate diffusion MR phantoms," in *ISMRM*, 2014.

[20] Y. Assaf and P. J. Basser, "Composite hindered and restricted model of diffusion (CHARMED) MR imaging of the human brain," *NeuroImage*, vol. 27, no. 1, pp. 48–58, 2005.

[21] M.-A. Côté, G. Girard, A. Boré, E. Garyfallidis, J.-C. Houde, and M. Descoteaux, "Tractometer: Towards validation of tractography pipelines," *Med Image Anal*, vol. 17, no. 7, pp. 844–57, 2013.

[22] J.-D. Tournier, F. Calamante, and A. Connelly, "MRtrix: Diffusion tractography in crossing fiber regions," *International Journal of Imaging Systems and Technology*, vol. 22, no. 1, pp. 53–66, 2012.

[23] J.-D. Tournier, F. Calamante, and A. Connelly, "Robust determination of the fibre orientation distribution in diffusion MRI: Non-negativity constrained super-resolved spherical deconvolution," *NeuroImage*, vol. 35, pp. 1459–1472, may 2007.

[24] J.-D. Tournier, F. Calamante, and A. Connelly, "Improved probabilistic streamlines tractography by 2nd order integration over fibre orientation distributions.," *Proceedings of the International Society for Magnetic Resonance in Medicine*, vol. 88, no. 2003, p. 2010, 2010.

[25] E. Kaden, F. Kruggel, and D. C. Alexander, "Quantitative mapping of the per-axon diffusion coefficients in brain white matter," *Magnetic Resonance in Medicine*, vol. 75, no. 4, pp. 1752–63, 2016.

[26] E. Kaden, N. D. Kelm, R. P. Carson, M. D. Does, and D. C. Alexander, "Multi-compartment microscopic diffusion imaging," *NeuroImage*, vol. 139, pp. 346–59, 2016.